

Supporting Information for

**NiCo<sub>2</sub>O<sub>4</sub>@Polyaniline Nanotubes Heterostructure  
Anchored on Carbon Textiles with Enhanced  
Electrochemical Performance for Supercapacitor  
Application**

Chenhao Pan,<sup>§†</sup> Zhaohui Liu,<sup>§†</sup> Wen Li,<sup>†\*</sup> Yunpeng Zhuang,<sup>†</sup> Qi Wang,<sup>†</sup> Shougang Chen<sup>†\*</sup>

<sup>†</sup>School of Material Science and Engineering, Ocean University of China, Qingdao, 266100, China

\*Corresponding authors

Shougang Chen (Tel: +86-0532-66781688; Email: [oucsgchen@163.com](mailto:oucsgchen@163.com))

Wen Li (Tel: +86-18354277550; Email: [wenli0720@gmail.com](mailto:wenli0720@gmail.com))

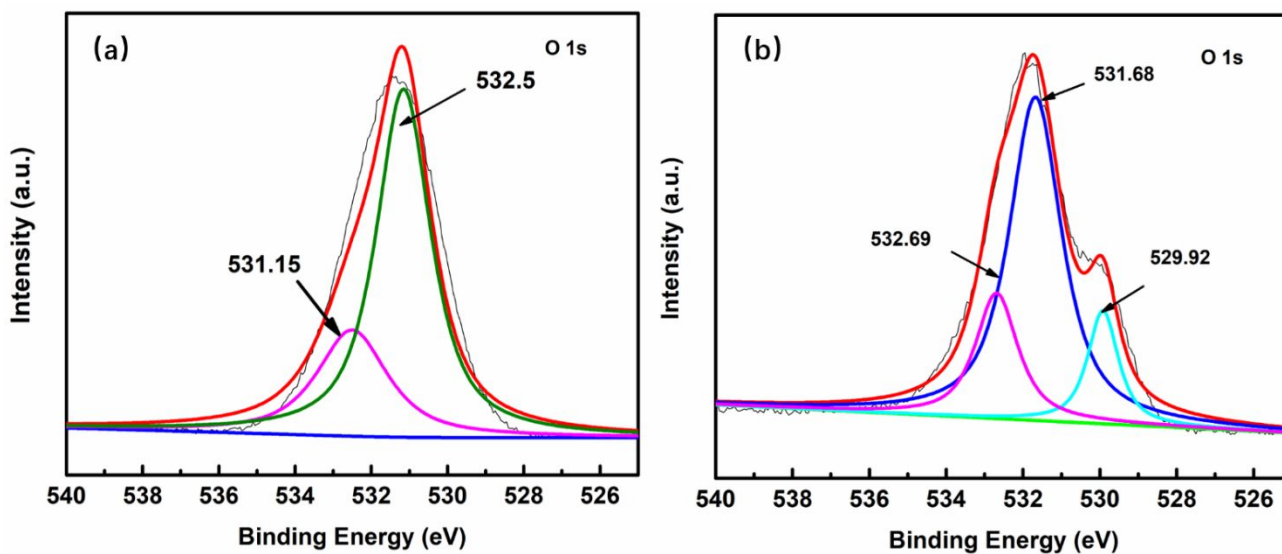


Figure S1. XPS spectra of O 1s for the NiCo<sub>2</sub>O<sub>4</sub>@PANI(a) and NiCo<sub>2</sub>O<sub>4</sub> (b).

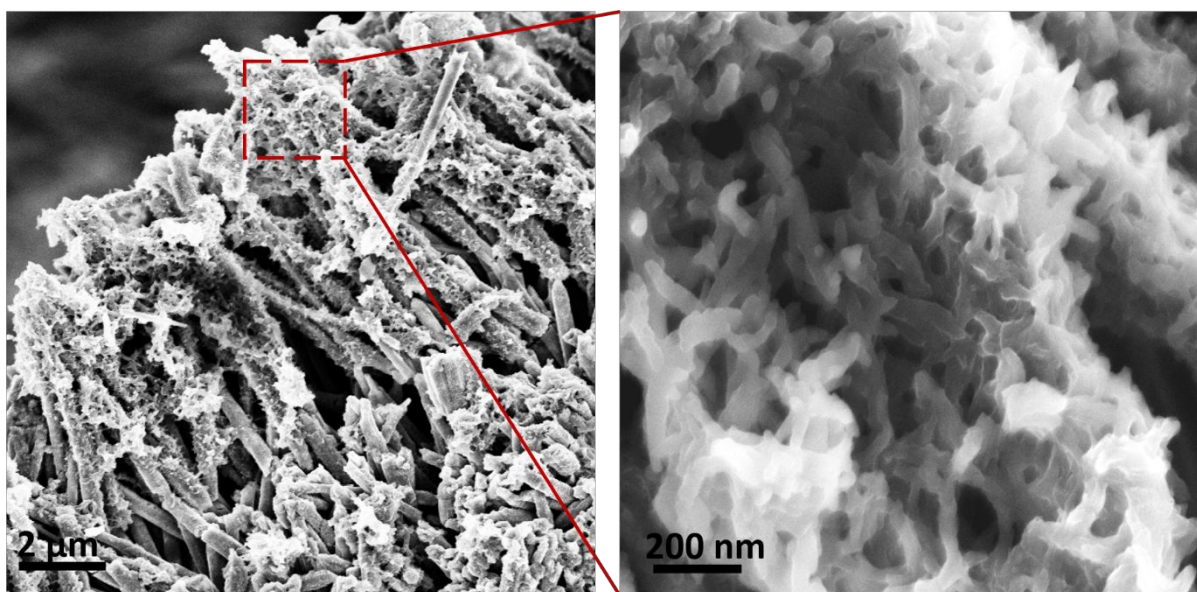
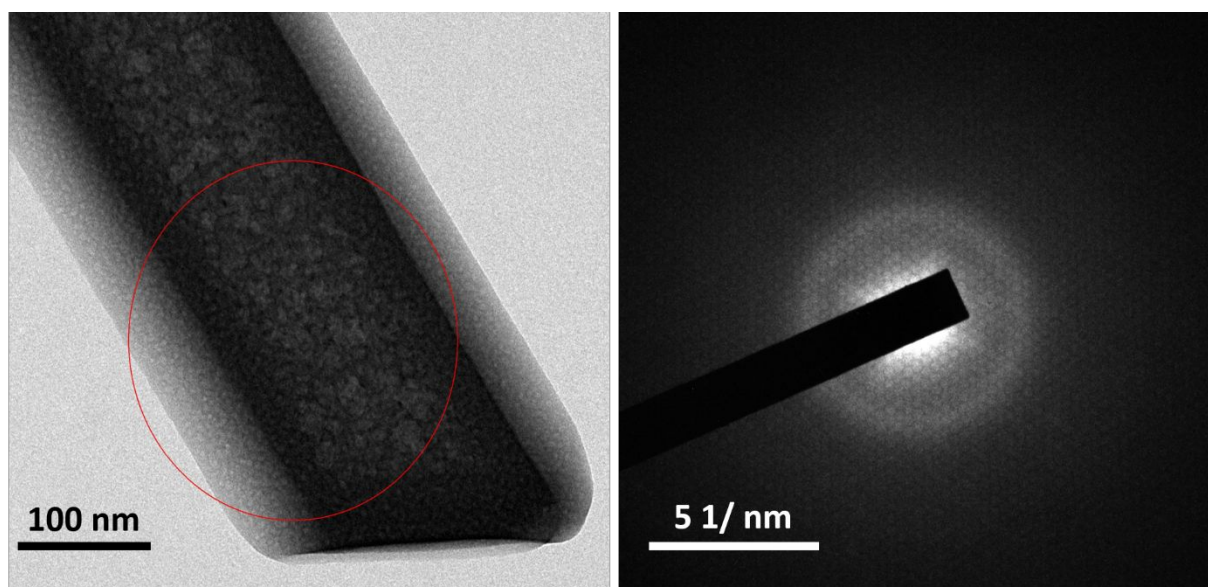
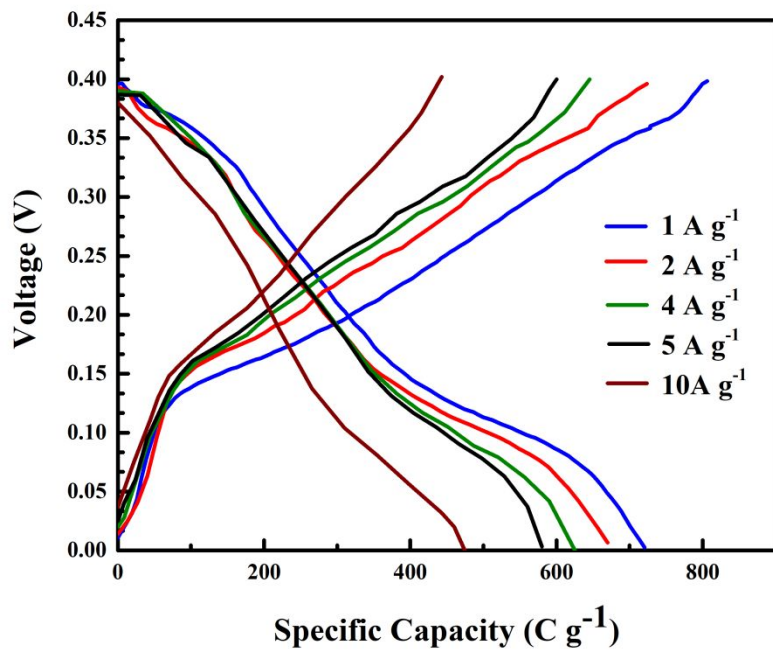


Figure S2. SEM images of the PANI nanofiber network on the surface of the NiCo<sub>2</sub>O<sub>4</sub> nanotube.



**Figure S3.** HRTEM images and corresponding FFT pattern of PANI membrane on the surface of nanotubes



**Figure S4.** Voltage/Capacity curves of NiCo<sub>2</sub>O<sub>4</sub>@PANI at different current densities.

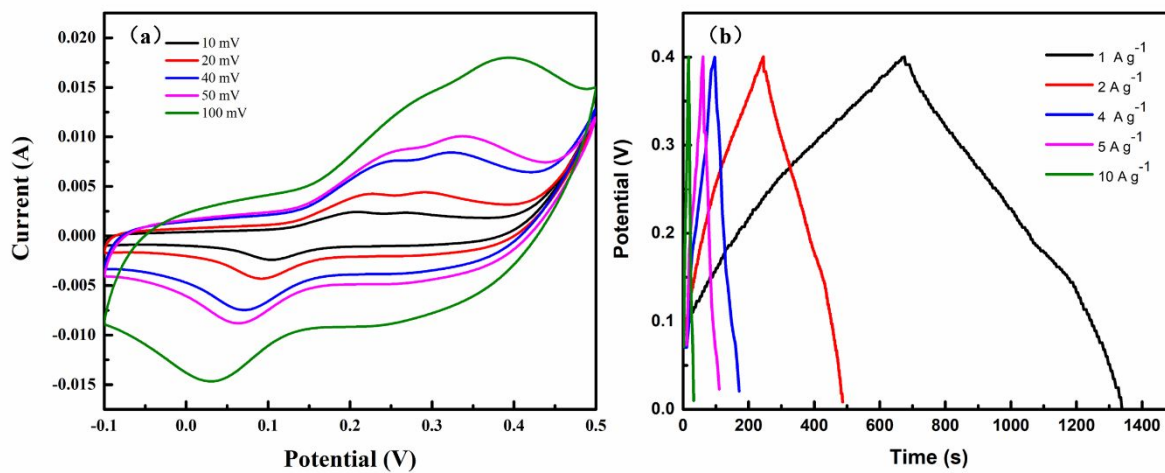


**Figure S5.** CV curves from 5 to 100 mVs<sup>-1</sup> and GCD curves at various current density of NiCo<sub>2</sub>O<sub>4</sub> sample.

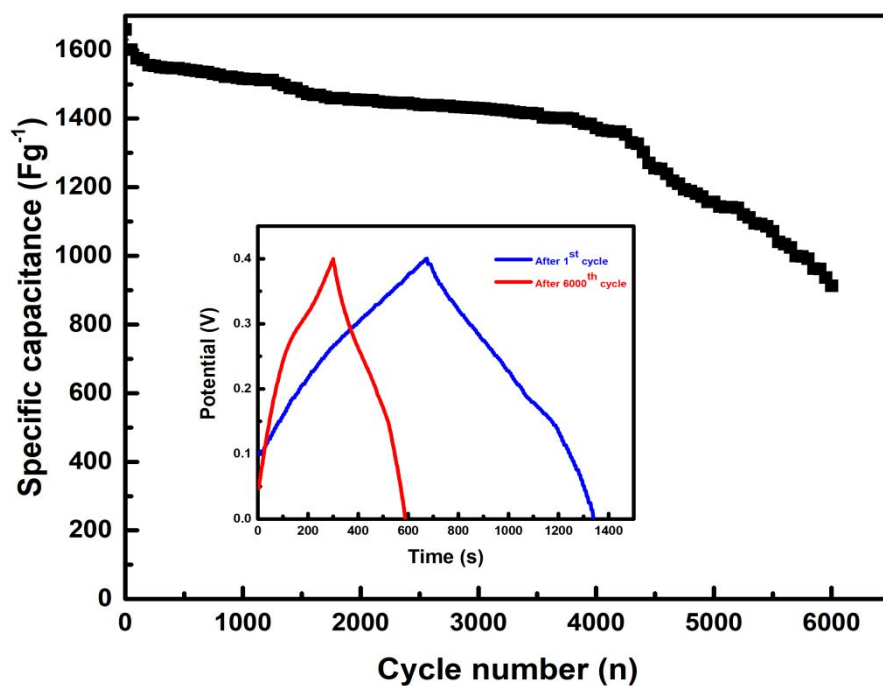
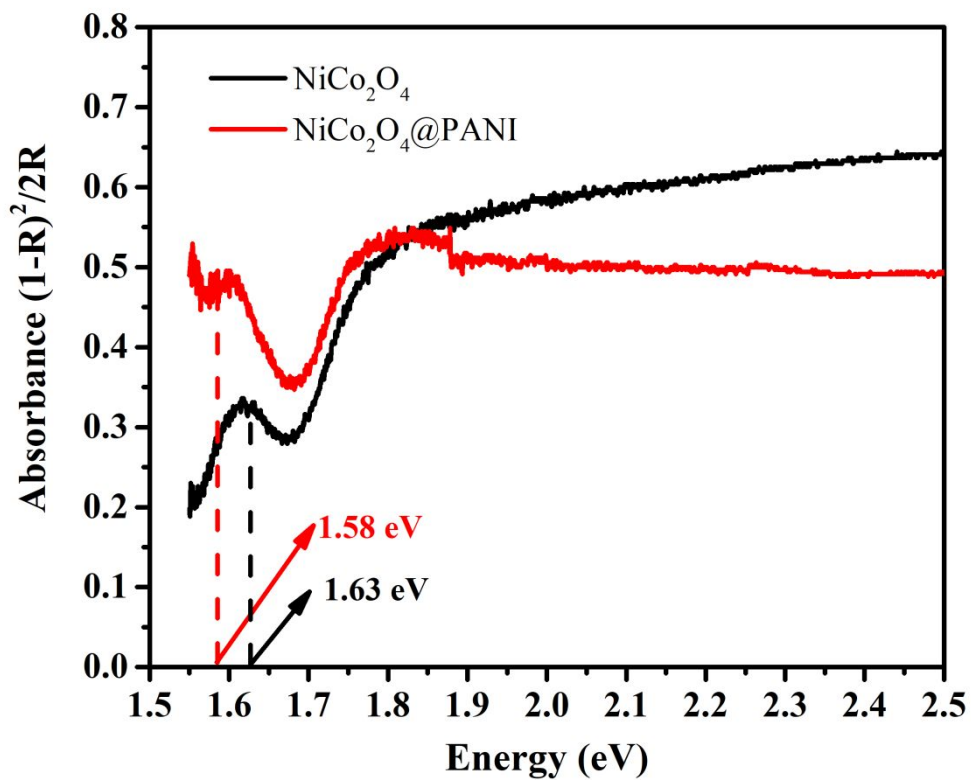


Figure S6. cycling performance at current densities of  $1 \text{ A g}^{-1}$  of  $\text{NiCo}_2\text{O}_4$  sample after 6000 cycles.



**Figure S7.** Kubelka-Munk transformed diffuse reflectance spectrum of NiCo<sub>2</sub>O<sub>4</sub> and NiCo<sub>2</sub>O<sub>4</sub>@PANI samples

### Dunn Method Analysis:

According to Dunn et al.<sup>1</sup>, we have analyzed cyclic voltammetry experiment data at different scan rates for NiCo<sub>2</sub>O<sub>4</sub>@PANI and NiCo<sub>2</sub>O<sub>4</sub> to study the different energy storage mechanisms. Because the charge storage processes can be separated to capacitive and diffusion-controlled contribution, it can be distinguished by fitting the relation between the peak current(*i*) and the scan rate(*v*) to the Eq.S1,

$$i = av^b \quad \text{Eq. S1}$$

where *a* and *b* are constants for certain electrochemical processes and *b* values(0.5~1) indicates the mechanism. When *b* coming to 0.5 indicates the diffusion-controlled behavior, while it approaching to 1 implies surface-controlled pseudocapacitive process.

To have a further insight on the mechanisms at play during the whole voltammetry curve, we can use the concepts mentioned above to deconvolute the two components corresponding two limiting situation and express the total current response at a certain potential as being the sum of two separate mechanisms, surface capacitive effects and diffusion-controlled insertion processes<sup>2</sup>:

$$i(V) = k_1v + k_2v^{1/2} \quad \text{Eq.S2}$$

where  $i(V)$  is the total current at the fixed potential  $V$  among the potential window,  $k_1v$  stands for surface capacitive process showing a linear dependence of the scan rate, while pure diffusion-controlled faradaic processes will show a linear dependence of the square root of the scan rate. Thus, the percentage of pseudocapacitive contribution is quantitatively determined by obtaining  $k_1$  and  $k_2$  values.

**Table S1. Comparison of the Electrochemical Performance of the NiCo<sub>2</sub>O<sub>4</sub>@PANI Electrode with that of Previously Reported Electrodes**

Material	Surface morphology	Capacitance	Current density	Electrolyte	Cycling performance	Reference
Ni <sub>0.67</sub> Co <sub>0.33</sub> MoO <sub>4</sub>	rod-like	441 C g <sup>-1</sup>	1 A g <sup>-1</sup>	6 M KOH	76.2 % after 1000 cycles	3
Co <sub>3</sub> O <sub>4</sub> @NiCo <sub>2</sub> O <sub>4</sub>	nanowires	9.12 F cm <sup>-2</sup>	2mAcm <sup>-2</sup>	2 M KOH		4
rGO/ NiCo <sub>2</sub> O <sub>4</sub>	nanowires	1248 F g <sup>-1</sup>	2mAcm <sup>-2</sup>		90% over 2000 cycles	5
NiCo <sub>2</sub> O <sub>4</sub>	nanowire arrays	1642 F g <sup>-1</sup>	1 A g <sup>-1</sup>	6 M KOH	95.7% after 10000 cycles	6
Ppy@ NiCo <sub>2</sub> S <sub>4</sub>	heterostructure	908.1 F g <sup>-1</sup>	1 A g <sup>-1</sup>	2 M KOH	87.7% after 2000 cycles	7
carbon spheres/ NiCo <sub>2</sub> O <sub>4</sub>	spheres	920 F g <sup>-1</sup>	1 A g <sup>-1</sup>	6 M KOH	87.9% after 2000 cycles	8
Co <sub>3</sub> O <sub>4</sub>	nanoflakes	576.8 C g <sup>-1</sup>	1 A g <sup>-1</sup>	2 M KOH	82% after 5000 cycles	9



NiCo <sub>2-x</sub> Fe <sub>x</sub> O <sub>4</sub>	Nanotubes	2057 F g <sup>-1</sup>	1 A g <sup>-1</sup>	6 M KOH	90.32% after 3000 cycles	10
Carbon fibers/ NiCo <sub>2</sub> O <sub>4</sub>	Nanosheets	1221 F g <sup>-1</sup>	1 A g <sup>-1</sup>	2 M KOH	81% after 3000 cycles	11
Co <sub>3</sub> O <sub>4</sub> @PPy	Nanorod arrays	1.02 F cm <sup>-2</sup>	1.5 mA cm <sup>-2</sup>	6 M KOH	10,000 cycles	12
NiCo <sub>2</sub> O <sub>4</sub> @PANI	Nanotube arrays	720.5 C g <sup>-1</sup>	1 A g <sup>-1</sup>	6 M KOH	99.64% after 10000 cycles	This work

---

## REFERENCES

- 1 Wang, J.; Polleux, J.; Lim, J.; Dunn, B. Pseudocapacitive Contributions to Electrochemical Energy Storage in TiO<sub>2</sub>(Anatase) Nanoparticles. *J. Phys. Chem. C* **2007**, *111* (40), 14925–14931.
- 2 León-Reyes, Á.; Epifani, M.; Chávez-Capilla, T.; Palmal, J.; Díaz, R. Analysis of the Different Mechanisms of Electrochemical Energy Storage in Magnetite Nanoparticles. *Int. J. Electrochem. Sci.* **2014**, *9* (7), 3837–3845.

- 3 Chen, H.; Chen, S.; Zhu, Y.; Li, C.; Fan, M.; Chen, D.; Tian, G.; Shu, K. Synergistic Effect of Ni and Co Ions on Molybdates for Superior Electrochemical Performance. *Electrochim. Acta* **2016**, *190*, 57–63.
- 4 Lu, Y.; Li, L.; Chen, D.; Shen, G. Nanowire-Assembled Co<sub>3</sub>O<sub>4</sub>@NiCo<sub>2</sub>O<sub>4</sub> Architectures for High Performance All-Solid-State Asymmetric Supercapacitors. *J. Mater. Chem. A* **2017**, *5*(47), 24981–24988.
- 5 Zhang, C.; Lei, C.; Cen, C.; Tang, S.; Deng, M.; Li, Y.; Du, Y. Interface Polarization Matters: Enhancing Supercapacitor Performance of Spinel NiCo<sub>2</sub>O<sub>4</sub> Nanowires by Reduced Graphene Oxide Coating. *Electrochim. Acta* **2018**, *260*, 814–822.
- 6 Qiu, W.; Xiao, H.; Yu, M.; Li, Y.; Lu, X. Surface Modulation of NiCo<sub>2</sub>O<sub>4</sub> Nanowire Arrays with Significantly Enhanced Reactivity for Ultrahigh-Energy Supercapacitors. *Chem. Eng. J.* **2018**, *352*, 996–1003.
- 7 Zheng, Y.; Xu, J.; Yang, X.; Zhang, Y.; Shang, Y.; Hu, X. Decoration NiCo<sub>2</sub>S<sub>4</sub>nanoflakes onto Ppy Nanotubes as Core-Shell Heterostructure Material for High-Performance Asymmetric Supercapacitor. *Chem. Eng. J.* **2018**, *333*(September 2017), 111–121.
- 8 Xu, Z.; Yang, L.; Jin, Q.; Hu, Z. Improved Capacitance of NiCo<sub>2</sub>O<sub>4</sub>/Carbon Composite Resulted from Carbon Matrix with Multilayered Graphene. *Electrochim. Acta* **2019**, *295*, 376–383.

- 9 Kong, S.; Yang, F.; Cheng, K.; Ouyang, T.; Ye, K.; Wang, G.; Cao, D. In-Situ Growth of Cobalt Oxide Nanoflakes from Cobalt Nanosheet on Nickel Foam for Battery-Type Supercapacitors with High Specific Capacity. *J. Electroanal. Chem.* **2017**, *785*, 103–108.
- 10 Liu, Z.; Wang, L.; Cheng, Y. F.; Cheng, X.; Lin, B.; Yue, L.; Chen, S. Facile Synthesis of NiCo<sub>2-x</sub>Fe<sub>x</sub>O<sub>4</sub> Nanotubes/Carbon Textiles Composites for High-Performance Electrochemical Energy Storage Devices. *ACS Appl. Nano Mater.* **2018**, *1* (2), 997–1002.
- 11 Zhang, J. N.; Liu, P.; Jin, C.; Jin, L. N.; Bian, S. W.; Zhu, Q.; Wang, B. Flexible Three-Dimensional Carbon Cloth/Carbon Fibers/NiCo<sub>2</sub>O<sub>4</sub> composite Electrode Materials for High-Performance All-Solid-State Electrochemical Capacitors. *Electrochim. Acta* **2017**, *256*, 90–99.
- 12 Wu, X.; Meng, L.; Wang, Q.; Zhang, W.; Wang, Y. A Flexible Asymmetric Fibered-Supercapacitor Based on Unique Co<sub>3</sub>O<sub>4</sub>@PPy Core-Shell Nanorod Arrays Electrode. *Chem. Eng. J.* **2017**, *327*, 193–201.